Effects of atmospheric turbulence on remote optimal control experiments

J. Extermann, P. Béjot, L. Bonacina,[a] P. Billaud, J. Kasparian,[b] and J.-P. Wolf
Université de Genève, GAP-Biophotonics, 20 rue de l'Ecole de Médecine, 1211 Geneva 4, Switzerland

Distortions of ultrashort laser pulses propagating through turbulence are investigated both experimentally and numerically. As expected, a strong correlation is found between temporal distortions and local intensity on the speckle pattern. We suggest that the localization of distortions in low-intensity regions may favor remote control strategies based on nonlinear interactions with respect to those based on linear schemes. © *2008 American Institute of Physics.*
[DOI: 10.1063/1.2838308]

Atmospheric applications of ultrashort and ultraintense lasers have recently emerged as a novel and very active field of research. On one side, the use of filamentation in air as coherent white light source for Light Detection and Ranging of atmospheric species has been proven as an attractive method.[1,2] On the other side, time-resolved and coherent control schemes have recently been used to efficiently discriminate between aerosol particles that exhibit identical spectral signatures.[3,4] There is now a particular interest to apply control schemes, such as fluorescence depletion and multipulse impulsive Raman spectroscopy,[5] directly in the atmosphere, especially since first field applications were demonstrated within the Teramobile project.[1,6] However, transmitting an optimally shaped pulse over long distance through the atmosphere is not fully straightforward. Although optimal control can be used to control filamentation in the field,[7] no demonstration of the applicability of quantum control of molecular species at a distance has been reported yet. Among the processes that may affect the propagation of an ultrashort laser pulse, thermal turbulence is likely the most effective in preventing remote control techniques. In fact, contrary to dispersion and Kerr-related effects, distortions induced by turbulence cannot be avoided by a sensible choice of the pulse characteristics, or precompensated,[8,9] due to their random nature. Pointing variation and wavefront distortions (speckles) of nanosecond or cw laser beams induced by atmospheric turbulence have been extensively studied.[10] In this paper, we investigate both experimentally and numerically how turbulence affects the properties of linearly propagating femtosecond laser pulses.

The measurements were carried out under stable environmental conditions (relative humidity $\leq 40\%$, temperature of 20 °C) with an amplified 1 KHz Ti:sapphire laser system delivering 2.5 mJ, 30 fs pulses with a beam diameter of ~ 12 mm at $1/e^2$ and curvature radius $R = -15$ m. After propagating over a distance of $d_1 = 3.8$ m, the beam goes across a highly turbulent region generated by the perpendicular flow of a hot air blower ($T \leq 500$ °C with 500 l/min flux, output air velocity of 20 m/s, angular divergence of 20°). The perturbation intensity is controlled by varying the distance between the blower and the beam axis. The strength of the perturbation, represented by the structure parameter of the refractive index C_n^2, was determined by measuring the

variance in pointing angle of a He–Ne laser collinear with the femtosecond beam.[11] The turbulence range achievable by the experiment $[C_n^2 = (7-15) \times 10^{-9} \text{ m}^{-2/3}]$ represents a very strong perturbation, a few orders of magnitude higher than those typically encountered in the atmosphere.[12] After passing through the turbulent region, the pulses propagate for an additional distance $d_2 = 3.7$ m before being characterized by a single shot autocorrelator (by sampling a 28 mm^2 portion in the center of the beam profile) or imaged by a digital charge coupled device camera equipped with a $f = 105$ mm objective (spatial resolution 150 μm/pixel, 10 ms exposure time). Alternatively, we characterized individual wavefront regions (0.25 mm^2) by frequency resolved optical gating (FROG) inserting in the beam path a random phase plate. This time-invariant perturbation allowed multishot acquisition. We measured by interferometry that the plate introduces an average phase difference of $\sim 4\pi/3$ among two points on the wavefront separated by 2 mm, an analogous estimate for a perturbation strength of $C_n^2 = 9.6 \times 10^{-10} \text{ m}^{-2/3}$ gives $\sim 2\pi/3$.

To complement the experimental measurements, we numerically simulated the propagation of a linearly polarized Gaussian pulse centered at $\lambda_0 = 800$ nm with wavefront curvature and radii matching the experimental values. Every spectral component is first propagated in free space, supposed to be linear and homogeneous, along a distance d_1. Then, to simulate the passage through turbulence, we apply a phase screen generated according to the Kolmogorov theory[13] for the different C_n^2 values. Finally, the pulse spectral components are propagated again in free space for an additional distance d_2.

As shown in Figs. 1(a) (experiment) and 1(b) (simulation), the beam profile is spatially distorted in a typical speckle pattern as a result of the propagation through turbulence. The experimental and simulated wavefronts bear a strong resemblance, especially considering that the former is the superposition of ten successive laser shots. The strongly inhomogeneous distribution of intensity, ranging from 10^{-3} to 2 times that of the unperturbed wavefront, results from the superposition of the multiple interferences among beam portions experiencing different phase shifts through turbulence repeated at each wavelength in the bandwidth.[14] Beside spatial distortions, we investigated also global temporal modifications, as reported in Fig. 1(c). Pulse autocorrelation widths averaged over 50 independent laser shots show a clear increase with turbulence strength. The experimental datapoints (squares) are normalized by the duration of a pulse propagating the same distance in the unperturbed laboratory atmo-
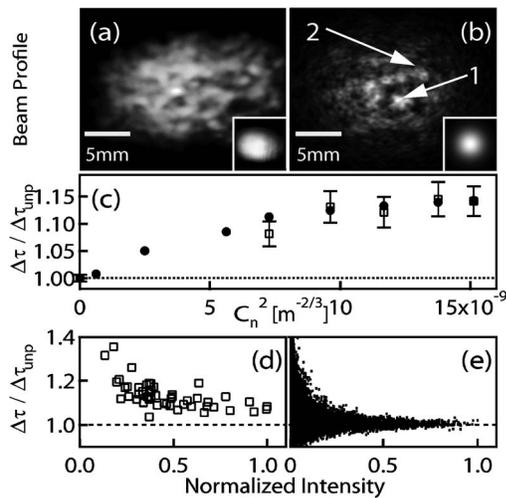
FIG. 1. (a) Experimental and (b) simulated beam profile. Arrows indicate the (1) strong and (2) the weak intensity spots. In the insets, the beam profiles in absence of artificial turbulence. (c) Pulse duration normalized to that of a pulse propagating the same distance in absence of turbulence as a function of turbulence strength, from experiment (□) and simulation (●). Relative pulse duration as a function of pulse intensity at fixed $C_n^2 = 9.6 \times 10^{-10}$ m$^{-2/3}$ from experiment (D) and simulation (E).

sphere, $\Delta\tau_{\text{unp}}$. Note that this duration does not correspond to that of a Fourier limited pulse. We derived from the simulation a comparable quantity by calculating the average of the temporal second moment of different beam portions normalized by the unperturbed value (circles). Note that, even in presence of strong perturbations, the average relative variation $\Delta\tau/\Delta\tau_{\text{unp}}$ does not exceed 15%. The quantitative agreement between experiment and calculations over the whole range of turbulence strengths investigated, authorizes to extend the simulations to the $C_n^2 = (2-7) \times 10^{-9}$ m$^{-2/3}$ range, which was not accessible in the experiment.

Figs. 1(d) and 1(e) compare the results of experiment and simulation by plotting the relative distortion of pulse duration as a function of the local wavefront intensity. The observed temporal distortions are strongly correlated with intensity, evidencing that the major deviations from the unperturbed case are concentrated in weak intensity regions. Pulse duration converges to the unperturbed one ($\Delta\tau/\Delta\tau_{\text{unp}} = 1$) as intensity increases.

We can gather more insight by investigating locally the spectral and temporal characteristics of regions of different intensities on the beam profile. As mentioned above, these measurements required the use of a random phase plate, which entails a much higher distortion than that generated by the hot air blow. In Fig. 2, we report two illustrative experimental temporal $[I(t)]$ and spectral $[I(\lambda)]$ profiles retrieved by inverting multishots FROG measurements from regions of different intensities: high [(a), (c)] and low [(b), (d)]. Similarly, Fig. 3 displays characteristic examples of simulated $I(t)$, $I(\lambda)$, and Wigner plot of strong [(a), (c), and (e)] and of weak [(b), (d), and (f)] intensity regions. The inspection of these traces further confirms the strong correlation between local intensity and pulse distortions. In low-intensity regions, the existence of substructures in the temporal profiles and major spectral alterations is clearly apparent from the plots. Conversely, for high intensities, little or no distortions are present and the traces almost perfectly overlap with those calculated for a pulse propagating in the
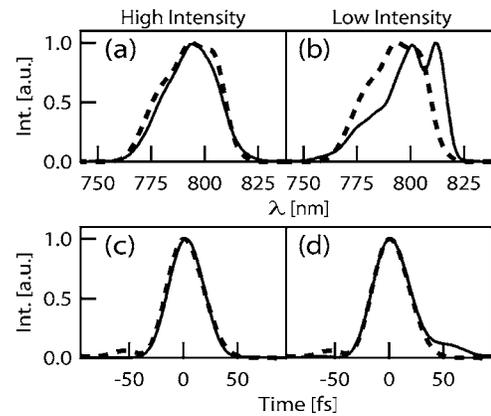

FIG. 2. Solid lines: experimental $I(\lambda)$ and $I(t)$ retrieved inverting the multi shot FROG measurement of [(a) and (c)] high and [(b) and (d)] weak intensity spots on the wavefront. Dotted lines: corresponding traces for a pulse propagating without turbulence over the same distance.

absence of turbulence (dotted lines). Simulation allowed us to determine that in the intense spots, the effect of multiple interferences accounts for minor amplitude deviations in both $I(t)$ and $I(\lambda)$, not exceeding a few percent fraction of the relative intensity. These observations altogether are consistent with a scenario where interferences act similarly at all wavelengths: in a defined portion of the beam profile, the spectral components experience a similar phase shift when passing through turbulence. Such a condition holds exclusively because of the narrow bandwidth of the femtosecond laser pulse (35 nm) as compared with the wavelength dependence of the index of refraction of air, n_{air}.

By integrating $I(t)$ across the beam profile, we conclude that the *overall* pulse duration is only slightly affected by turbulence: 6% on the temporal second moment with respect to the unperturbed situation for $C_n^2 = 9.6 \times 10^{-10}$ m$^{-2/3}$. This C_n^2 value is four orders of magnitude higher than typical atmospheric conditions. In the approximation of constant tur-
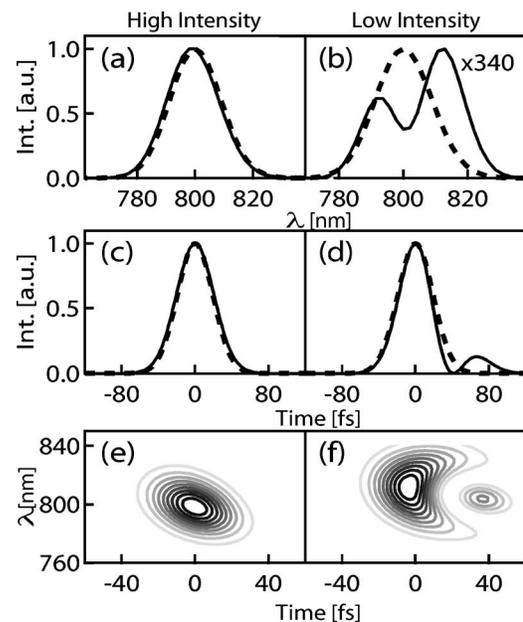

FIG. 3. [(a) and (b)] Simulated $I(\lambda)$, [(c) and (d)] $I(t)$, and [(e) and (f)] Wigner representation of the pulse characteristics in the high (left column) and low (right column) intensity spots on the beam profiles indicated by arrows 1 and 2 in Fig. 1(b).

bulence over the propagation length,[15] using a standard value[12] for strong atmospheric turbulence ($C_n^2 = 2.5 \times 10^{-13}$ m$^{-2/3}$), we can extrapolate that comparable pulse distortions should appear after kilometric propagation. However, the strong assumptions prevent a more quantitative estimation.

To conclude, the effect of atmospheric turbulence on linearly propagating femtosecond laser pulses can be simply treated as the superposition of interferences independently acting on the components of the pulse spectrum. Bright spots on the wavefront correspond to weakly perturbed regions, which essentially maintain the spectral and temporal properties of the original pulse. The degree of alteration anticipated for actual atmospheric propagation ($<6\%$) does not constitute an overwhelming limitation but it is a factor to take into account to design robust remote control applications. A partial compensation to the effects of turbulence can be achieved by adopting control strategies based on multiple-photon interactions, as nonlinear power dependence limits higher order interactions within intense beam regions, where the original spectral and temporal pulse features are conserved. In analogy with what is currently done in astronomy,[16] one can also envisage to use adaptive optical components to realize real-time wavefront correction; taking into consideration the weak spectral dependence over pulse bandwidth of n_{air}, we suggest that this way not only spatial but also temporal distortions of femtosecond pulses can be actively compensated for.

[1] J. Kasparian, M. Rodriguez, G. Mejean, J. Yu, E. Salmon, H. Wille, R. Bourayou, S. Frey, Y. B. Andre, A. Mysyrowicz, R. Sauerbrey, J. P. Wolf, and L. Woste, Science **301**, 61 (2003).

[2] H. L. Xu, J. F. Daigle, Q. Luo, and S. L. Chin, Appl. Phys. B: Lasers Opt. **82**, 655 (2006).

[3] F. Courvoisier, V. Boutou, V. Wood, A. Bartelt, M. Roth, H. Rabitz, and J. P. Wolf, Appl. Phys. Lett. **87**, 063901 (2005).

[4] F. Courvoisier, V. Boutou, L. Guyon, M. Roth, H. Rabitz, and J. P. Wolf, J. Photochem. Photobiol., A **180**, 300 (2006).

[5] D. Pestov, R. K. Murawski, G. O. Ariunbold, X. Wang, M. C. Zhi, A. V. Sokolov, V. A. Sautenkov, Y. V. Rostovtsev, A. Dogariu, Y. Huang, and M. O. Scully, Science **316**, 265 (2007).

[6] G. Mejean, J. Kasparian, E. Salmon, J. Yu, J. P. Wolf, R. Bourayou, R. Sauerbrey, M. Rodriguez, L. Woste, H. Lehmann, B. Stecklum, U. Laux, J. Eisloffel, A. Scholz, and A. P. Hatzes, Appl. Phys. B: Lasers Opt. **77**, 357 (2003).

[7] R. Ackermann, E. Salmon, N. Lascoux, J. Kasparian, P. Rohwetter, K. Stelmaszczyk, S. H. Li, A. Lindinger, L. Woste, P. Bejot, L. Bonacina, and J. P. Wolf, Appl. Phys. Lett. **89**, 171117 (2006).

[8] H. Wille, M. Rodriguez, J. Kasparian, D. Mondelain, J. Yu, A. Mysyrowicz, R. Sauerbrey, J. P. Wolf, and L. Woste, Eur. Phys. J.: Appl. Phys. **20**, 183 (2002).

[9] I. Pastirk, X. Zhu, R. M. Martin, and M. Dantus, Opt. Express **14**, 8885 (2006).

[10] J. Goodman, *Statistical Optics* (Wiley, New York, 2000).

[11] R. Ackermann, G. Mejean, J. Kasparian, J. Yu, E. Salmon, and J. P. Wolf, Opt. Lett. **31**, 86 (2006).

[12] S. Bendersky, N. S. Kopeika, and N. Blaunstein, Appl. Opt. **43**, 4070 (2004).

[13] C. M. Harding, R. A. Johnston, and R. G. Lane, Appl. Opt. **38**, 2161 (1999).

[14] W. J. Liu and C. H. Zhou, Appl. Opt. **44**, 6506 (2005).

[15] R. Salamé, N. Lascoux, E. Salmon, R. Ackermann, J. Kasparian, and J.-P. Wolf, Appl. Phys. Lett. **91**, 171106 (2007).

[16] R. Foy, A. Migus, F. Biraben, G. Grynberg, P. R. McCullough, and M. Tallon, Astron. Astrophys. Suppl. Ser. **111**, 569 (1995).